THE LANCET Infectious Diseases

Supplementary webappendix

This webappendix formed part of the original submission and has been peer reviewed. We post it as supplied by the authors.

Supplement to: Griffin JT, Bhatt S, Sinka ME, et al. Potential for reduction of burden and local elimination of malaria by reducing Plasmodium falciparum malaria transmission: a mathematical modelling study. *Lancet Infect Dis* 2016; published online Jan 19. http://dx.doi.org/10.1016/S1473-3099(15)00423-5.

The potential for burden reduction and local elimination achievable with reducing *Plasmodium falciparum* transmission: a modelling study.

Supplementary Information

JT Griffin[1,2] PhD, S Bhatt[4] DPhil, ME Sinka[4] PhD, PW Gething[4] PhD, M Lynch[3] MD, E Patouillard[3,5,6] PhD, E Shutes[3] MPH, RD Newman[3] MD, Professor P Alonso[3] MD, RE Cibulskis[3] PhD, Professor AC Ghani PhD[1*]

1. *MRC Centre for Outbreak Analysis & Modelling, Imperial College London*
2. *School of Mathematical Sciences, Queen Mary University of London*
3. *Global Malaria Programme, WHO*
4. *Spatial Ecology and Epidemiology Group, Department of Zoology, University of Oxford*
5. *Swiss Tropical and Public Health Institute*
6. *Universität Basel*

The model described here is an extension of a model published in 2010 by Griffin et al.[1] and subsequently re-fitted to capture the relationship between exposure and clinical disease [2] and severe disease and death.[3] It has been further extended to capture the mosquito dynamics as described in White et al.[4] The full current model is described in Section 1. The model includes multiple malaria interventions. Extensions made to these intervention models are detailed in Section 2. Section 3 gives further details of the geographically explicit parameters and Section 4 summarises the approach taken to obtain uncertainty intervals. In Section 5 we provide links to additional movies showing the changing map of *P.falciparum* malaria under the scenarios outlined in the main manuscript.

1 *P.falciparum* transmission model

The model is described in its deterministic framework here. However, for the simulation results modelling multiple interventions, it was implemented as an equivalent stochastic individual-based model. The only change to this structure in the stochastic version is the non-exponential durations of protection after treatment described in Section 3.

Susceptible individuals (S) are infected at a rate Λ which depends on the entomological inoculation rate (EIR). After a fixed 12 day latent period, they either develop symptoms (with probability ϕ) or proceed with asymptomatic infection (state A). The probability of developing symptoms, ϕ, is determined by an individual's level of exposure-drive immunity (see below) which changes through the course of their lifetime. Those developing disease are either successfully treated (entering state T) or fail treatment or are untreated (entering state D). Those that are successfully treated subsequently enter a period of prophylaxis (P) with the duration of this state depending on the drug used. Following this, individuals return to the susceptible state S. Those that fail treatment or are not treated are assumed to self-resolve and become asymptomatic (entering state A). As only a small proportion of cases are fatal (see Section 2) we do not explicitly model deaths in the transmission cycle. Individuals with asymptomatic infection subsequently move to a sub-patent state (U) which

allows the model to capture onward infection from individuals with low parasite densities. Super-infection can occur from states A and U. All states are also stratified by the rate at which people are bitten by mosquitoes to capture heterogeneity in exposure.

The differential equations for the human transmission model are as follows:

$$\frac{\partial S}{\partial t}+\frac{\partial S}{\partial a}+\frac{\partial S}{\partial \zeta}=-\Lambda S+P/d_P+U/d_U$$
$$\frac{\partial T}{\partial t}+\frac{\partial T}{\partial a}+\frac{\partial T}{\partial \zeta}=\phi f_T\Lambda(S+A+U)-T/d_T$$
$$\frac{\partial D}{\partial t}+\frac{\partial D}{\partial a}+\frac{\partial D}{\partial \zeta}=\phi(1-f_T)\Lambda(S+A+U)-D/d_D$$
$$\frac{\partial A}{\partial t}+\frac{\partial A}{\partial a}+\frac{\partial A}{\partial \zeta}=(1-\phi)\Lambda(S+U)+D/d_D-\phi\Lambda A-A/d_A$$
$$\frac{\partial U}{\partial t}+\frac{\partial U}{\partial a}+\frac{\partial U}{\partial \zeta}=A/d_A-U/d_U-\Lambda U$$
$$\frac{\partial P}{\partial t}+\frac{\partial P}{\partial a}+\frac{\partial P}{\partial \zeta}=T/d_T-P/d_P$$

where t denotes time, a denotes age and ξ denotes the biting rate on an individual (capturing heterogeneity in exposure). Here f_T is the proportion of clinical cases receiving effective treatment and d_T, d_D, d_A, d_P, d_U denote the mean duration of states T, D, A, P and U respectively.

Variation in exposure to mosquitoes is included to capture both increased biting with age and other sources of heterogeneity in exposure (for example, geographic variation). Each individual has a relative biting rate ζ which is drawn from a Log-Normal distribution with parameters $-\sigma^2/2$ and σ, such that ζ has a mean of 1. If ε_0 is the mean EIR in adults, then the EIR (ε) and force of infection (Λ) at age a are given by the equations:

$$\varepsilon=\varepsilon_0\zeta\left(1-\rho\exp(-a/a_0)\right)$$
$$\Lambda=\varepsilon b$$

where b is the probability of infection if bitten by an infectious mosquito, and ρ and a_0 determine how the rate of being bitten changes with age.

1.1 Acquisition and decay in naturally acquired immunity

To capture the natural acquisition of immunity to malaria disease and infection, we define four empirical functions that apply at different stages of human infection:

- *Pre-erythrocytic immunity,* I_B*:* this is assumed to reduce the probability of infection if bitten by an infectious mosquito;
- Acquired and maternal clinical immunity, I_{CA} and I_{CM} respectively: the effect of blood stage immunity in reducing the probability of developing clinical symptoms;
- *Acquired and maternal immunity to severe disease:* Similar quantities I_{VA} and I_{VM} reducing the probability of severe malaria;
- *Detection immunity,* I_D*:* the effect of blood stage immunity in reducing the detectability of an infection and onward transmission to mosquitoes.

Each of the four acquired immunity functions are assumed to change with exposure as follows, starting from zero at birth:

$$\frac{\partial I_B}{\partial t}+\frac{\partial I_B}{\partial a}=\frac{\varepsilon}{\varepsilon u_B+1}-I_B/d_B$$
$$\frac{\partial I_{CA}}{\partial t}+\frac{\partial I_{CA}}{\partial a}=\frac{\Lambda}{\Lambda u_C+1}-I_{CA}/d_C$$
$$\frac{\partial I_{VA}}{\partial t}+\frac{\partial I_{VA}}{\partial a}=\frac{\Lambda}{\Lambda u_V+1}-I_{VA}/d_V$$
$$\frac{\partial I_D}{\partial t}+\frac{\partial I_D}{\partial a}=\frac{\Lambda}{\Lambda u_D+1}-I_D/d_D$$

In each equation, $u_k, k=B,CA,\mathrm{VA},\mathrm{D}$ limits the rate at which immunity can be boosted at high exposure and each $d_k, k=B,C,V,D$ determines the duration of immunity.

The immunity functions are transformed by Hill functions to give the probabilities of each transition affected by immunity. The probability of infection decreases from b_0 with no

immunity to a minimum of $b_0 b_1$, and is given by the following formula where I_{B0} and κ_B are scale and shape parameters respectively:

$$b = b_0\left(b_1 + \frac{1-b_1}{1+\left(I_B / I_{B0}\right)^{\kappa_B}}\right)$$

At birth, maternal clinical immunity I_{CM} is P_M times the acquired immunity of a 20 year-old, then decays at rate $1/d_M$. The probability of clinical disease is ϕ_0 with no immunity, and has a minimum of $\phi_0\phi_1$, and is given by the following formula where I_{C0} and κ_C are scale and shape parameters respectively:

$$\phi = \phi_0\left(\phi_1 + \frac{1-\phi_1}{1+\left((I_{CA}+I_{CM})/I_{C0}\right)^{\kappa_C}}\right)$$

The probability of severe malaria if newly infected is similar, apart from an extra age-dependent term f_V:

$$\theta = \theta_0\left(\theta_1 + \frac{1-\theta_1}{1+f_V\left((I_{VA}+I_{VM})/I_{V0}\right)^{\kappa_V}}\right)$$

where $f_V = 1-(1-f_{V0})/\left(1+(a/a_V)^{\gamma_V}\right)$ at age a, with parameters f_{V0}, a_V and γ_V.

The probability of detecting an asymptomatic infection by microscopy is

$$q = d_1 + \frac{(1-d_{\min})}{\left(1+(I_D/I_{D0})^{\kappa_D} f_D\right)}$$

$d_{\min}$ is the minimum probability, I_{D0} and κ_D are scale and shape parameters, and $f_D = 1-(1-f_{D0})/\left(1+(a/a_D)^{\gamma_D}\right)$ at age a, with parameters f_{D0}, a_D and γ_D.

This reduced detectability is assumed to result from a lower parasite density, which also reduces the probability of infecting a mosquito if bitten. In states D and U, infectiousness is c_D and c_U respectively. Following treatment, infectivity is c_T. In state A, infectiousness is $c_U + (c_D - c_U)q^{\gamma_I}$ where q is the probability of detection of parasites.

The estimates of the central human transmission model parameters and their 95% credible intervals where fitted are given in Table S1. Full details and estimates of the parameters governing immunity are given in Griffin et al. 2014 and 2015.[5,6]

Table S1: Parameters for the baseline human transmission model.

Parameter	Symbol	Estimate (95% credible interval)
Human infection duration (days)		
Latent period	d_E	12 (fixed)
Patent infection	d_I	200 (fixed)
Clinical disease (treated)	d_T	5 (fixed)
Clinical disease (untreated)	d_D	5 (fixed)
Sub-patent infection	d_U	110 (87,131)
Prophylaxis following treatment	d_P	Based on drug PK/PD profile[7]
Infectiousness to mosquitoes		
Lag from parasites to infectious gametocytes	t_l	12.5 days (fixed)
Untreated disease	c_D	0.068 day^{-1}(0.039, 0.122)
Treated disease	c_T	Drug-dependent
Sub-patent infection	c_U	0.0062 day^{-1} (0.00056, 0.018)
Parameter for infectiousness of asymptomatic state	γ_I	1.82 (0.603, 8.54)
Age and heterogeneity		
Age-dependent biting parameter	ρ	0.85 (fixed)
Age-dependent biting parameter	a_0	8 years (fixed)
Variance of the log heterogeneity in biting rates	σ^2	1.67 (fixed)
Parameters determining immunity		
Probability that an infectious bite leads to infection	b	See Griffin et al. (2014) and (2015) for further details[5,6]
Probability that an infection leads to disease	ϕ	
Probability that an infection leads to severe disease	θ	
Probability that an infection will be detected	q	

1.2 Mortality

The model has previously been fitted to data on the incidence of severe malaria in different transmission settings as described in Griffin et al.[6]. This allows us to estimate the relative incidence and changing age distribution of severe malaria as transmission intensity varies from a wide range of African datasets and also obtain estimates of the case fatality in hospital using data from Tanzania. However there remains considerable uncertainty in the overall incidence of severe malaria (including those who do not reach hospital), and consequently in the case fatality of severe cases who do not reach hospital. To obtain an estimate of the overall mortality rate we therefore used data collated by Rowe et al.[8]. In that study, verbal autopsy data were used to estimate the relationship between reported estimates of parasite prevalence in children and mortality due to malaria in under-fives from the same location. The data were collected in the late 1980s and 1990s, prior to the widespread scale-up of intervention coverage.

The model described above predicts the incidence of hospitalised severe malaria at time t and age a, $\lambda_H(a,t) = \int_\zeta \Lambda(a,t,\zeta)\theta(a,t)\,\mathrm{d}\zeta$, where Λ is the force of infection, θ is the proportion of new infections that result in severe malaria and ζ is the heterogeneity in exposure. We assume that the overall mortality due to malaria $\mu(a,t)$ is proportional to the incidence of hospitalised severe malaria:

$$\mu(a,t) = \nu\lambda_H(a,t)$$

To estimate the scaling factor ν using the verbal autopsy data, we ran our simulation model with no long-lasting insecticide treated nets (LLINs) and the constant assumed treatment rate for each first administrative unit in Africa, and output the parasite prevalence in 2 to 10 year olds and hospitalised severe malaria incidence in under-fives. We then estimated ν by least squares, weighted by the population in each first administrative unit. The resulting estimate when using the best-fit transmission model parameters in Table S1 is that we

multiply the model-predicted incidence of hospitalised severe malaria in a given age group by ν = 0.215 to predict overall mortality due to malaria in the same age group. We re-estimated ν for each set of transmission model parameters when carrying out the uncertainty analysis described below.

When coverage of effective treatment is scaled up, this is likely to reduce the probability of progressing to severe malaria and death. We assume that effective treatment for uncomplicated malaria prevents a proportion χ of deaths. As there are no reliable data for this parameter, we sampled a value uniformly between 0 and 1. Suppose that the proportion of uncomplicated malaria cases that are effectively treated was historically f_0 and is now f_1. Then the incidence of severe malaria and mortality due to malaria are both multiplied by

$$\frac{(1-\chi)f_1+(1-f_1)}{(1-\chi)f_0+(1-f_0)}$$

relative to the incidence if treatment coverage remained at f_0.

1.3 Mosquito dynamics

The full lifecycle of the mosquito is modelled in a compartmental formulation[9]. Female adult mosquitoes (M) lay eggs at rate β which then develop through the early and late larval stages (E and L) to the pupal stage (P_L). The death rate of the larval stages is increased by a density-dependent factor. Pupae emerge as adult mosquitoes, with 50% being female, which are susceptible to infection (S_M). The differential equations are:

$$\frac{dE}{dt} = \beta M - \mu_E\left(1+\frac{E+L}{K}\right)E - \frac{E}{d_{EL}}$$
$$\frac{dL}{dt} = \frac{E}{d_{EL}} - \mu_L\left(1+\gamma\frac{E+L}{K}\right)L - \frac{L}{d_L}$$
$$\frac{dP_L}{dt} = \frac{L}{d_L} - \mu_P P_L - \frac{P_L}{d_{PL}}$$
$$\frac{dS_M}{dt} = \frac{P_L}{2d_{PL}} - \mu_M S_M$$

where each μ is a death rate, each d is the duration in a state, and γ modifies the effect of density dependence on late stage relative to early stage larvae. K is the time-varying carrying capacity, the ability of the environment to support mosquito larvae, which determines the mosquito density and hence the baseline transmission intensity in the absence of interventions.

Adult mosquitoes become infected at a rate which depends on the infectiousness of the human population, which in turn depends on the infection states at time t_l previously, where t_l represents the time lag in humans from asexual parasites to onward infectiousness. The force of infection on mosquitoes is the sum of the contributions from the different human infection states:

$$\Lambda_M = \frac{\alpha}{\omega}\int_0^\infty\int_0^\infty \zeta\psi(a)\left(c_D D(\zeta,a,t-t_l) + c_T T(\zeta,a,t-t_l) + c_A A(\zeta,a,t-t_l) + c_U U(\zeta,a,t-t_l)\right) da\, d\zeta$$

The biting rate on humans is $\alpha = Q_0/\delta$, where δ is the mean time between feeds and Q_0 is the proportion of bites that are on humans (anthropophagy). $\omega = \int_0^\infty \psi(a)g(a)\,da$ is a normalizing constant for the biting rate over ages, where $g(a)$ is the cross-sectional human age distribution.

Once infected, mosquitoes pass through a latent period (E_M) of fixed length τ_M and then they become infectious to humans (I_M). They are assumed to remain infectious until they die. The infection process in the mosquito population is as follows:

$$\frac{dS_M}{dt} = \frac{P_L}{2d_{PL}} - \Lambda_M S_M - \mu_M S_M$$
$$\frac{dE_M}{dt} = \Lambda_M S_M - \Lambda_M(t-\tau_M)S_M(t-\tau_M)P_M - \mu_M E_M$$
$$\frac{dI_M}{dt} = \Lambda_M(t-\tau_M)S_M(t-\tau_M)P_M - \mu_M I_M$$

where μ_M is the death rate and $P_M = e^{-\mu_M \tau_M}$ is the probability that a mosquito survives the extrinsic incubation period. The mean EIR for adult humans is then given by

$$\varepsilon_0 = I_M \alpha / \omega$$

The parameter values for the mosquito population model are given in

Table S2.

Table S2: Parameters for the mosquito population model.

Parameter	Symbol	Estimate
Daily mortality of adults	μ_M	Varies by species
Per capita daily mortality rate of early stage larvae (low density)	μ_E	0.034 day^{-1}
Per capita daily mortality rate of late stage larvae (low density)	μ_L	0.035 day^{-1}
Per capita daily mortality rate of pupae	μ_P	0.25 day^{-1}
Mean time between bites in humans	δ	3 days
Development time of early stage larvae	d_{EL}	6.64 days
Development time of late stage larvae	d_L	3.72 days
Development time of pupae	d_{PL}	0.64 days
Number of eggs laid per day per mosquito	β	21.19 day^{-1}
Relative effect of density dependence on late instars relative to early instars	γ	13.25
Extrinsic incubation period	τ_M	10 days

2 Intervention Models

2.1 Treatment for uncomplicated and severe malaria

When used as treatment for uncomplicated malaria, we assume that non-ACTs have a 75% probability of being effective in clearing an infection, whereas ACTs have a 95% probability of being effective.[1] If a drug is effective, then it also provides a period of prophylaxis with a profile of protection over time that differs for each drug, and also varies by age, as estimated for artemether/lumefantrine (AL) and DHA-piperaquine by Okell at al.[7] We assumed that ACTs have the properties of AL, and for non-ACTs, we assumed a 30 day duration of prophylaxis.[10]

Rectal artesunate given in the community was assumed to reduce progression to severe malaria by 50%.[11] Injectable artesunate as a treatment for severe malaria in hospital has a 23% efficacy in reducing mortality in under-fives and 35% efficacy in over fives compared to treatment with quinine[12,13] which is assumed to be the standard treatment in hospital before injectable artesunate is introduced.

2.2 Seasonal Malaria Chemoprevention

Seasonal malaria chemoprevention (SMC) consists of three courses of treatment (SP plus amodiaquine) during the transmission season. Treatment courses were given to the target population at the peak of the transmission season (as defined by the peak of the carrying capacity $K(t)$), and one month before and after the peak. We assumed that the drug was efficacious and provided a period of prophylaxis of approximately 30 days. SMC was implemented in sufficiently seasonal areas of sub-Saharan Africa, defined as areas with at least 60% of the rainfall occurring in the peak three months of the year, and where the incidence of clinical malaria in under-fives was at least 0.1 cases per person per year at baseline.[14] In the first and second acceleration scenarios, SMC was only implemented in the Sahel, as there is wide-spread resistance to sulfadoxine/pyrimethamine (SP) in East Africa. In the innovate scenario, SMC was also implemented in suitable areas of Africa outside the

Sahel, under the assumption that a drug combination would be available that could be used for SMC where there is currently SP resistance.

2.3 Vector Control

LLINs and IRS are modelled as described in Griffin et al. (2010)[1] apart from one change to the intervention model structure, which was that now we allow the possibility that IRS kills a mosquito as it rests in a house before feeding. Both interventions are modelled by calculating the probabilities that a mosquito trying to feed is killed, repelled or successfully feeds. These probabilities were based on an updated literature review of experimental hut studies (manuscript in preparation), and are listed in Table S3. The endophily parameters for *Anopheles gambiae ss*, *arabiensis* and *funestus* in Table S5 were also based on this updated review.

Table S3: Parameters for the effects of LLINs and IRS

	Probability of being:	Symbol	Value
LLINs	Repelled before entering house	r_E	0.113
	Repelled by net	r_P	0.295
	Killed by net	d_N	0.533
IRS	Repelled before entering house	r_I	0.687
	Killed before feeding	d_{IW}	0.295

3 Country-specific Parameters

3.1 Vector species and behaviour

For each country, we identified the three most important dominant vector species. Within Africa, we used a published model based on rainfall and humidity to estimate the relative density of two of the dominant species (*An.gambiae s.s.* and *An.arabiensis*).[15] In areas where the third dominant species (*An.funestus*) is also present, we assumed that this represented 20% of the total vector population. This assumption has relatively little impact on the outcomes as the effectiveness of LLINs and IRS is most impacted by the density of *An.arabiensis*.

Outside Africa, the dominant vector species were taken from estimates of their presence/absence.[16-19] Up to three dominant species were identified in each country, and then the proportions that each species represent out of the total mosquito numbers were given the values in Table S4, dependent on how many dominant species there were.

Table S4: Parameters assumed for the relative density of the three dominant vector species in each country

	Relative proportion of each species		
	Species 1	Species 2	Species 3
Three dominant species	0.6	0.3	0.2
Two dominant species	0.6	0.4	-
One dominant species	1	-	-

The parameters for vector behaviour that determine the impact of LLINs and IRS are shown in Table S5. The quantity of data on these traits varies by species and for many is not available. Hence we took two different approaches inside and outside Africa. For the three dominant species in Africa we used estimates for each of these traits (apart from endophily) from the literature, as in our previous work.[1] For each species outside Africa we first

calculated the proportion of papers that reported each species to have any of these four traits based on the information published in the bionomics references.[16-19] Next, we used a threshold to turn these reports into binary outcomes – high and low – for each trait. This threshold was set at a level which best represented the overall split in the data for each trait (close to 50% for the first 3 traits and 75% for the last trait). Finally, we assigned fixed numerical values for each trait for a high/low level, based on data from *An.gambiae s.s* (high anthropophagy, endophily, endophagy and proportion of bites indoors when people are in bed) and *An.arabiensis* (low anthropophagy and endophily), but less endophagic than *An.arabiensis*.

Table S5: Bionomics of the categorised vector species

Trait	An.gambiae s.s	An.arabiensis	An.funestus	"High"	"Low"
Anthropophagy	0.92	0.71	0.94	0.9	0.6
Endophily	0.813	0.422	0.813	0.85	0.3
% bites indoors	0.97	0.96	0.98	0.96	0.6
% bites indoors and in bed	0.89	0.9	0.9	0.9	0.5

3.2 Demographic and parasite prevalence data

The total population in each country by year and the changing age distribution were based on the UN World Population Projections, which consist of data up to 2012, and projections from 2013 onwards.[20] The data included estimates of the population by 5-year age-groups, infant mortality, and the birth rate per person. Annual population data were available, whereas yearly infant mortality and birth rates were interpolated from five-yearly data. Population growth was considered separately for urban and rural areas, as these differ due to trends in urbanisation. Estimates of the population spatial distribution in 2010 within each country at a resolution of 1km^2 were taken from GRUMP.[21] As the country totals for these population estimates do not necessarily match the UN data perfectly, the populations were first rescaled so that the total in each country matched the UN 2010 data.

The baseline transmission intensity is based on estimates of parasite prevalence in 2 to 10 year olds in 2010 from the Malaria Atlas Project (MAP).[22] These estimates were made based on data from 22,212 *P.falciparum* parasite rate surveys. We combined these data with the demographic data to calculate, for each first administrative unit, the mean *P. falciparum* parasite prevalence weighted by population, and the total population and the population living in areas with stable transmission of *P. falciparum* (referred to in the main text as the population at risk). The calculations were undertaken separately for urban and rural areas.

For calculation of incidence of cases and deaths, the denominator population was taken as the total population in first administrative areas which were malaria-endemic in 2010. The growth in the population of these areas over the period 2015 to 2030 is projected to be 25% overall, with 44% growth in Africa, 15% in Asia and the Pacific, and 15% in Latin America. The projected growth in urban populations is 71%, 40% and 22% respectively, whereas the growth in rural populations is 27%, 2% and -4%.

In the main text we report changes in case incidence and mortality. These are per population statistics and hence are not influenced by population growth. We also report absolute numbers of cases and deaths averted as these statistics are commonly used in reporting. It should be noted that these numbers do capture the substantial population growth outlined above.

3.3 Calibration of baseline transmission intensity

The carrying capacity of the environment to support mosquito larvae, $K(t)$, is assumed to be proportional to rainfall. A seasonal curve was estimated from daily rainfall data from 2002 to 2009 using the first three frequencies of the Fourier-transformed data as detailed in Garske et al.[23], and the results were aggregated to the first administrative units. Let $R(t)$ be this rainfall curve, with mean over the year of $\bar{R}$. To calibrate the model to match the MAP 2010 parasite prevalence data, we repeatedly ran the deterministic transmission model over

50 years up to 2010 within a root-finding algorithm, using the site-specific data on vectors, LLIN scale-up and treatment for clinical malaria. The seasonal carrying capacity is taken as

$$K(t) = K_0 R(t) / \bar{R}$$

with K_0 varying at each iteration of the root-finding procedure until a value of K_0 which gives the desired prevalence in 2010 is found. This calibration was done separately for urban and rural populations in each first administrative area. We assumed that apart from seasonal variation, $K(t)$ remains constant over time, so that with a growing human population, in the absence of interventions, the mosquito density per person decreases.

Outside Africa, and in Botswana, Namibia, South Africa and Madagascar, there was an additional calibration step, rescaling all values of K_0 within each country (by a single factor per country) so that the number of clinical malaria cases in 2010 matched the number estimated by the WHO, as summarised in the 2013 World Malaria Report (WMR).[24] In these countries, we assumed that the minimum incidence of clinical malaria in 2010 among the at-risk population was 1 case per 100 people per year. To achieve this, where necessary we decreased the population at risk from that derived from the MAP and demographic data, while still matching the total number of cases in each countries as estimated by the WHO.

3.4 Coverage of interventions from 2000 to 2015

3.4.1 LLIN Coverage

For LLINs we define coverage as usage of nets, as measured frequently in DHS/MIS surveys. LLIN usage in sub-Saharan Africa was estimated from a model which was jointly fitted to data on numbers of nets delivered to countries and data from household surveys of ownership and use of LLINs.[25] The model provides estimates of the proportion of the population who sleep under an LLIN in each country by year from 2000 to 2013. Outside

Africa we used National Malaria Control Program reports of LLIN usage collated by WHO/GMP from 2000 to 2012 and reported for recent years in the WMR 2013.

In our simulation model, we assume that nets are distributed every three years to up to one third of the population (all-age to reflect the policy of universal coverage), and that after people receive a new net, usage falls at a constant rate with a mean duration of usage of 5 years. For each country, we numerically found the set of annual distribution coverages that, with our simulation assumptions, most closely match the usage estimates, by minimising the sum of squares of the difference between the annual usages output from our simulation and the annual usages from the distribution/ownership model or WHO data.

For the “Sustain” scenario the LLIN usage, weighted by population of malaria-endemic areas, has a median value of 42% (interquartile range 6-60%). The other scenarios have a target access level, where usage is 88% of access as estimated in Bhatt et al. [25]

3.4.2 IRS Coverage

For IRS we define coverage as the proportion of people residing in a house that has been sprayed within the past 12 months. Data on IRS coverage by country was taken from the WMR 2013 which collates coverage reported from the National Malaria Control Programmes. For the “Sustain” scenario the LLIN coverage, weighted by population of malaria-endemic areas, has a median value of 11% (interquartile range 1-19%). IRS coverage is not continued in scenarios two, three and four since we model vector control via LLINs only.

3.4.3 SMC Coverage

For SMC we define coverage as the proportion of children residing in an area suitable for SMC that receive the full 3 courses of SP-amodiaquine. We do not model partial adherence to this schedule. SMC is not included in the “Sustain” scenario.

3.4.4 Treatment Coverage

For first-line treatment for uncomplicated malaria (clinical disease) we define coverage as the proportion of those that develop disease that receive a full course of an appropriate and efficacious drug (either non-ACT or ACT – see section 2.1. This coverage figure therefore encompasses treatment seeking, appropriate diagnosis, the availability of ACTs and adherence to the dosing schedule. The complexities of this treatment seeking pathway are not explicitly modelled here given the wide variation within and between countries. Instead this is reflected in country-specific coverage estimates.

In Africa, antimalarial and ACT coverage (i.e. the proportion receiving either a non-ACT or ACT) plus the proportion of these treatments received in the public versus private sector were based on modelled estimates from DHS and MICS surveys reported in Cohen et al. [26]. Outside Africa we used data from the WMR 2013 which is reported by the National Malaria Control Programmes. The latter coverage levels reflect treatment in the public sector only. In the absence of further data we therefore assumed that coverage levels would be 50% lower in the private sector compared to the public sector. Data on the proportion of cases seeking care in the public and private sectors was obtained from the WMR 2013 as reported by National Malaria Control Programmes.

For the “Sustain” scenario the first-line treatment coverage, weighted by population of malaria-endemic areas, has a median value of 36% (interquartile range 31-40%).

Data on case management rates for severe disease (i.e. the proportion of severe disease cases that receive hospital care) are limited. For a given transmission setting, we previously estimated severe malaria incidence in hospital λ_H and incidence of mortality due to malaria, $\mu = \nu\lambda_H$, with ν estimated as described in section 1.2. We also have an estimate of the case fatality of hospitalised severe malaria, m_H of 0.065, based on the study of Reyburn et al.[27] To estimate the overall incidence of severe malaria, we took the case fatality outside hospital

m_C to be 0.6, based on the review by Lubell at al.[28] Then to reconcile these estimates, the incidence of non-hospitalised severe malaria λ_C must satisfy

$$m_H \lambda_H + m_C \lambda_C = \mu = \nu \lambda_H$$
$$\lambda_C = \frac{(\nu - m_H)}{m_C} \lambda_H$$

In scenarios three and four, rectal artesunate in the community reduces m_C , and in scenarios two, three and four, injectable artesunate in hospital reduces m_H .

4 Simulations and Uncertainty Analysis

Simulations were run separately in urban and rural populations in each first administrative unit, with no spatial linking of transmission between them. The size of the simulated populations ranged from 12,000 for the places with highest transmission to 60,000 at low transmission. Each simulation was run for 50 years prior to 2015.

When we fitted the transmission model to data as described in [5,6], we used a Bayesian framework, thus obtaining a posterior distribution of parameter sets. From these, we chose 50 sets of parameters at random. For each set of parameters, we repeated the calibration of the baseline transmission intensity in each country and first administrative unit. Uncertainty in the vector bionomics was included by sampling each of the parameters listed in Table S5 from a Logit Normal distribution with median equal to the value in the table and standard deviation on the logit scale of 0.4 in Africa and 0.8 outside Africa. For each of the 50 parameter sets, we also repeated the rescaling to the mortality data estimated by verbal autopsy and sampled the rescaling parameter ν from a gamma distribution with mean equal to the fitted value and standard deviation equal to the standard error from the fitting of ν.

We then ran each simulation scenario for all 50 sets of parameters. For each result in the main text, the point estimate is the mean over the 50 simulation runs, after aggregating over countries, and over years where necessary. Approximate 95% credible intervals were calculated by fitting a three parameter distribution to the outputs from the 50 simulations using maximum likelihood, and calculating the 2.5th and 97.5th percentiles of the fitted distribution. The distributions chosen were a generalised gamma distribution for outcomes that must be non-negative, such as the number of cases or deaths, and a skew-normal distribution for outcomes that could be positive or negative, such as the relative or absolute change in cases or deaths.

5 Additional explanation of rebounds

As shown in Figure 1 of the main text, under the “sustain” scenario in which coverage of interventions remains at 2013 level, we predict a small rebound in case incidence and mortality. This is due to a reduction in the rate of acquisition of immunity in younger children that are exposed at a lower level and hence a shifting in cases to older ages. As we demonstrate here, this is not unique to malaria but is the expected outcome of any intervention that reduces the hazard of infection and hence results in a later age at first (and subsequent) infections.

To illustrate this, we use a very simple example of multiple birth cohorts experiencing a fully-immunising infection. Assume that each child experiences a constant risk of infection from 2000 to 2009 which then decreases to a lower level from 2010 onwards, as illustrated in Figure S1. All children are assumed to survive throughout.

Figure S1: Scenario with a reduced risk of infection from 2009 onwards.

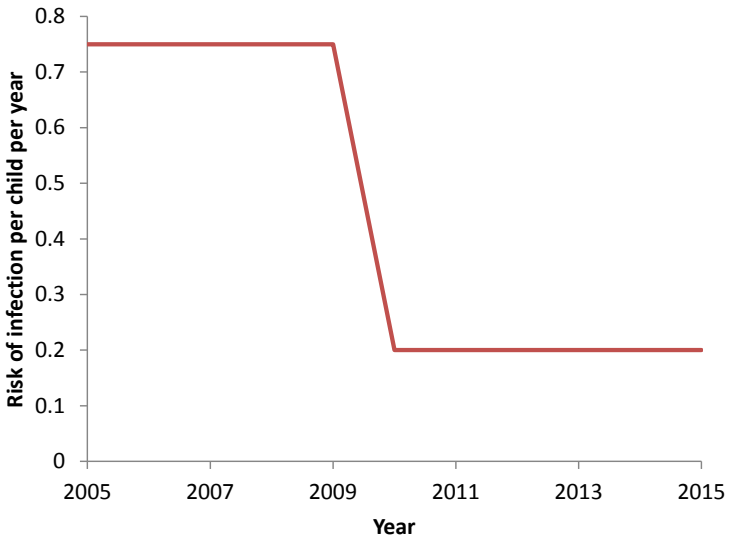

To further simplify, assume that the infection always results in disease and that the child is then fully immune following this single infection. Figure S2 shows the cumulative probability

of having been infected by age in four cohorts of children. In those born in the year 2000, the high risk of infection means that the majority are infected early in life with almost all having experienced infection by the age of 5. A similar pattern is observed for those born in 2005. However, now we see a flattening of the curve from age 4 onwards as those that have not been infected by 2009 (the year in which transmission decreases) acquire infection at a slower rate. Of those born in 2008 a large proportion are infected in their first year of life, but after this the rate of acquisition of infection is slower, reflecting the reduced risk of infection from 2009 onwards. Finally, the 2010 and all later cohorts acquire infection at a slower rate as they are exposed only to the lower risk of infection throughout their life.

Figure S2: The cumulative probability of acquiring infection by age for four different cohorts.

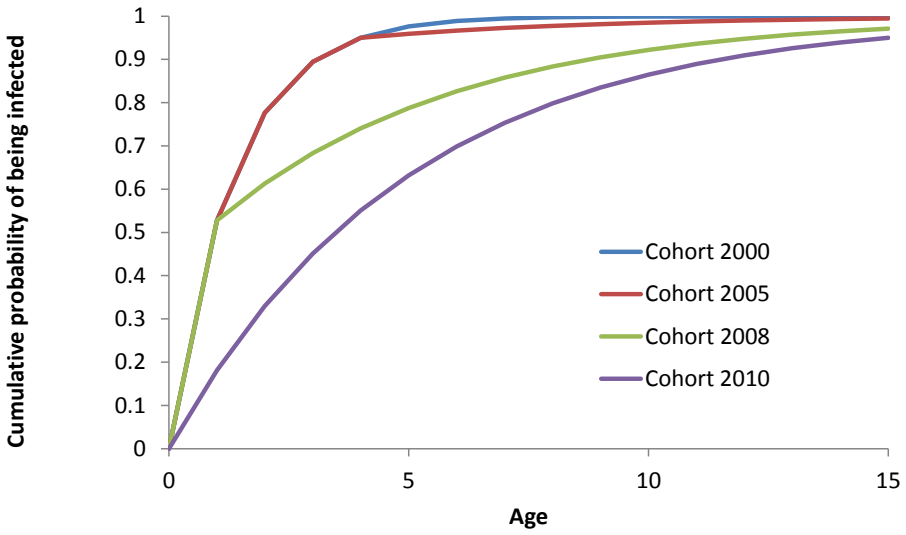

The reduction in infection risk from 2009 therefore results in an increase in the average age of first infection for the later cohorts compared with the baseline situation (represented by the 2005 cohort). This effect explains the increase in age of cases that has been observed in many malaria endemic settings as transmission declines.

In addition, Figure S2 shows how the probability of acquiring infection by age 10 decreases in each cohort, representing an absolute reduction in risk over an individual's lifetime. This is further illustrated in Figure S3, which shows the age distribution of the cases by cohort.

Figure 3: Age distribution of cases in children under 5 years by cohort. The later cohorts experience a lower risk of infection and hence cases are shifted to older ages.

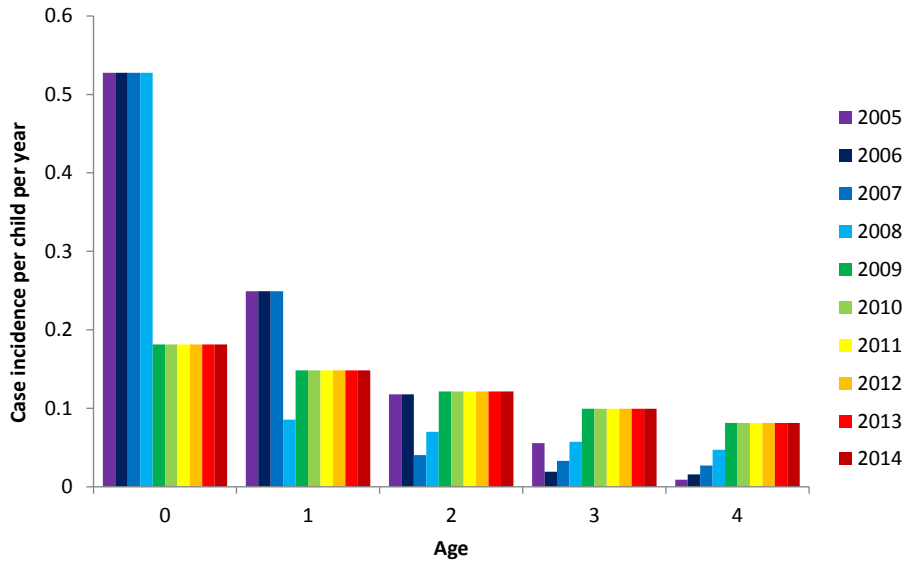

Figure S4 shows how the same data in Figure S3 can be re-plotted with calendar year along the x-axis to demonstrate the contribution of the different cohorts to overall case incidence in children under 5 years of age. In each bar, the top segment represents 0 year olds, the second bar 1 year olds, the third 2 year olds etc. In 2007 and 2008 the proportion of cases in each age-group is constant. Following the 2009 decrease in infection risk, the case incidence in the 0 year olds (2009 cohort) is smaller than that in 2007/2008. Notably, the number of cases occurring in 2009 in the 2007 and 2008 cohorts (navy and dark blue respectively) is low as most of the children in these cohorts have experienced their infection. As the new cohorts emerge, children experience their infection at older ages and so these new cases give rise to an increase in the overall case incidence. However the total risk of infection in the later cohorts is always lower than in the earlier cohorts.

Figure S4: (A) Contribution of cohorts to the total case incidence in children under 5 years of age. The colours denote the cohorts of children born from 2003 to 2015. (B) Summary trajectory of case incidence in children under 5 years of age.

(A) **(B)**

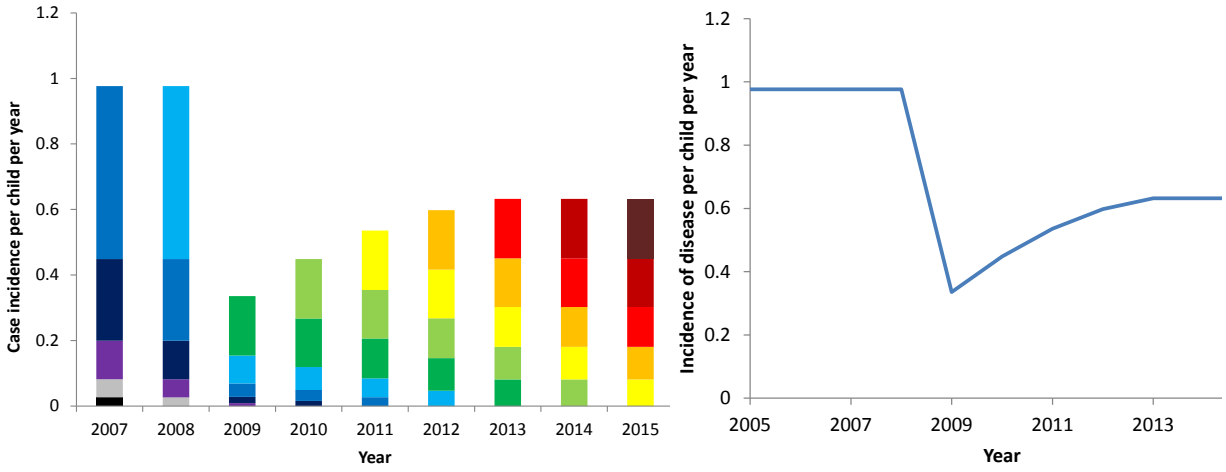

6 Additional Maps and Movies

The following movies show the yearly output of the model from 2010 to 2030.

Movie S1: Changing map of *P.falciparum* under the Sustain scenario.

Movie S2: Changing map of *P.falciparum* under the Accelerate 1 scenario.

Movie S3: Changing map of *P.falciparum* under the Accelerate 2 scenario.

Movie S4: Changing map of *P.falciparum* under the Innovate scenario.

Movie S5: Changing map of *P.falciparum* under the Reverse scenario.

7 References

1. Griffin JT, Hollingsworth TD, Okell LC, et al. Reducing Plasmodium falciparum malaria transmission in Africa: a model-based evaluation of intervention strategies. *PLoS Med* 2010; **7**(8).

2. Griffin JT, Ferguson NM, Ghani AC. Who gets sick with malaria? A method to estimate the relationship between prevalence of infection and incidence of disease accounting for the changing age-profile of cases. *In preparation* 2012.

3. Griffin JT, Hollingsworth TD, Reyburn H, Drakeley CJ, Riley EM, Ghani AC. Gradual acquisition of immunity to severe malaria with increasing exposure. *Proc Biol Sci* 2015; **282**(1801).

4. White MT, Griffin JT, Churcher TS, Ferguson NM, Basanez MG, Ghani AC. Modelling the impact of vector control interventions on Anopheles gambiae population dynamics. *Parasit Vectors* 2011; **4**(1): 153.

5. Griffin JT, Ferguson NM, Ghani AC. Estimates of the changing age-burden of Plasmodium falciparum malaria disease in sub-Saharan Africa. *NATURE COMMUNICATIONS* 2014; **5**.

6. Griffin JT, Hollingsworth TD, Reyburn H, Drakeley CJ, Riley EM, Ghani AC. Gradual acquisition of immunity to severe malaria with increasing exposure. *Proceedings of the Royal Society B: Biological Sciences* 2015; **282**(1801): 20142657.

7. Okell LC, Cairns M, Griffin JT, et al. Contrasting benefits of different artemisinin combination therapies as first-line malaria treatments using model-based cost-effectiveness analysis. *NATURE COMMUNICATIONS* 2014; **5**.

8. Rowe AK, Rowe SY, Snow RW, et al. The burden of malaria mortality among African children in the year 2000. *Int J Epidemiol* 2006; **35**(3): 691-704.

9. White MT, Griffin JT, Churcher TS, Ferguson NM, Basanez MG, Ghani AC. Modelling the impact of vector control interventions on Anopheles gambiae population dynamics. *Parasit Vectors* 2011; **4**: 153.

10. Cairns M, Carneiro I, Milligan P, et al. Duration of Protection against Malaria and Anaemia Provided by Intermittent Preventive Treatment in Infants in Navrongo, Ghana. *PLoS ONE* 2008; **3**(5): e2227.

11. Gomes MF, Faiz MA, Gyapong JO, et al. Pre-referral rectal artesunate to prevent death and disability in severe malaria: a placebo-controlled trial. *The Lancet*; **373**(9663): 557-66.

12. Dondorp AM, Fanello CI, Hendriksen ICE, et al. Artesunate versus quinine in the treatment of severe falciparum malaria in African children (AQUAMAT): an open-label, randomised trial. *The Lancet*; **376**(9753): 1647-57.

13. Dondorp A, Nosten F, Stepniewska K, Day N, White N. Artesunate versus quinine for treatment of severe falciparum malaria: a randomised trial. *Lancet* 2004; **366**(9487): 717-25.
14. Cairns M, Roca-Feltrer A, Garske T, et al. Estimating the potential public health impact of seasonal malaria chemoprevention in African children. *Nat Commun* 2012; **3**: 881.
15. Lindsay S, Parson L, Thomas C. Mapping the range and relative abundance of the two principal African malaria vectors, Anopheles gambiae sensu stricto and An. arabiensis, using climate data. *Proceedings of the Royal Society of London Series B: Biological Sciences* 1998; **265**(1399): 847-54.
16. Sinka ME, Rubio-Palis Y, Manguin S, et al. The dominant Anopheles vectors of human malaria in the Americas: occurrence data, distribution maps and bionomic precis. *Parasit Vectors* 2010; **3**: 72.
17. Sinka ME, Bangs MJ, Manguin S, et al. A global map of dominant malaria vectors. *Parasit Vectors* 2012; **5**: 69.
18. Sinka ME, Bangs MJ, Manguin S, et al. The dominant Anopheles vectors of human malaria in Africa, Europe and the Middle East: occurrence data, distribution maps and bionomic precis. *Parasit Vectors* 2010; **3**: 117.
19. Sinka ME, Bangs MJ, Manguin S, et al. The dominant Anopheles vectors of human malaria in the Asia-Pacific region: occurrence data, distribution maps and bionomic precis. *Parasit Vectors* 2011; **4**: 89.
20. United Nations Department for Economic and Social Affairs. World Population Prospects, The 2012 Revision. 2013. http://esa.un.org/unpd/wpp/Excel-Data/population.htm.
21. Center for International Earth Science Information Network - CIESIN - Columbia University, International Food Policy Research Institute - IFPRI, The World Bank, Centro Internacional de Agricultura Tropical - CIAT. Global Rural-Urban Mapping Project, Version 2 (GPW-UR): Gridded Population of the World. Palisades, NY: NASA Socioeconomic Data and Applications Center (SEDAC); 2011.
22. Gething PW, Patil AP, Smith DL, et al. A new world malaria map: Plasmodium falciparum endemicity in 2010. *Malar J* 2011; **10**: 378.
23. Garske T, Ferguson NM, Ghani AC. Estimating air temperature and its influence on malaria transmission across Africa. *PLoS One* 2013; **8**(2): e56487.
24. World Health Organisation. World Malaria Report. 2013.
25. Bhatt S, Weiss DJ, Mappin B, et al. Insecticide-treated nets (ITNs) in Africa 2000-2017: coverage, system efficiency and future needs to achieve international targets. *e-Life* 2015: in press.
26. Cohen JM, Woolsey AM, Sabot OJ, Gething PW, Tatem AJ, Moonen B. Optimizing investments in malaria treatment and diagnosis. *Science* 2012; **338**(6107): 612-4.

27. Reyburn H, Mbatia R, Drakeley C, et al. Association of transmission intensity and age with clinical manifestations and case fatality of severe Plasmodium falciparum malaria. *JAMA* 2005; **293**(12): 1461-70.
28. Lubell Y, Staedke SG, Greenwood BM, et al. Likely health outcomes for untreated acute febrile illness in the tropics in decision and economic models; a Delphi survey. *PloS One* 2011; **6**(2): e17439.